

DEVELOPMENT AND CHARACTERIZATION OF SALICYLIC ACID-BASED MICROEMULSIONS FOR TOPICAL APPLICATION

MARINA-THEODORA TALIANU^{1,2}, CRISTINA-ELENA DINU-PÎRVU^{1,2},
 MIHAELA VIOLETA GHICA^{1,2,*}, VALENTINA ANUȚA^{1,2}, RĂZVAN MIHAI
 PRISADA^{1,2}, ANDREEA-DENISA COCIOABĂ^{1,2}, ELENA-DIANA CĂPĂTOIU^{1,2},
 RALUCA-ELENA GOIA^{1,2}, LĂCRĂMIOARA POPA^{1,2}

¹“Carol Davila” University of Medicine and Pharmacy, Faculty of Pharmacy, 6 Traian Vuia Str., 020956, Bucharest, Romania, Corresponding author: mihaela.ghica@umfd.ro

²Innovative Therapeutic Structures R&D Center (InnoTher), “Carol Davila” University of Medicine and Pharmacy, Bucharest, Romania

The goal of the study was to design topical microemulsions using salicylic acid as a poorly soluble model drug. The microemulsions were selected by building a pseudoternary phase diagram, starting from four main components namely oleic acid, Tween 80, propylene glycol, and ultrapure water. The systems were obtained by solubilizing salicylic acid into the oil and the stabilizer mixture (surfactant/co-surfactant – S/CoS), using water titration. Then, the following parameters were studied: pH, conductivity, refractive index, mean droplet size, rheological descriptors, and surface tension. The organoleptic properties were specific for the selected ingredients, and the pH values were considered appropriate for applying the microemulsion to the skin. The conductivity confirmed the microemulsion O/W type, while the refractive index values were specific for isotropic systems. The mean droplet size varied between 117-272 nm, under the influence of stabilizers, using two methods: the Cumulant model and the Sparse Bayesian Learning algorithm. The rheological analysis offered information related to the internal structure of microemulsions, characterized by Newtonian or non-Newtonian flow. The non-Newtonian behaviour was evaluated through Ostwald-de-Waele, and Herschel-Bulkley models respectively. The surface tension was specific for dispersions stabilized by adequate quantities of S/CoS and varied between 30.82-34.71 mN/m. The developed salicylic acid-based microemulsions presented adequate physico-chemical characteristics, making them promising solutions for treating certain dermatological disorders such as acne, psoriasis, or cutaneous keratosis.

Keywords: salicylic acid, topical microemulsions, physicochemical characteristics.

INTRODUCTION

In the actual context, an integrated approach to managing dermatologic conditions involves a rapid diagnosis and a targeted treatment to rebalance normal cutaneous metabolism (Zhang *et al.*, 2023). From the most encountered diseases diagnosed in different age groups, acne, psoriasis, cutaneous keratosis, and specific forms of dermatitis lead to imbalances in normal cellular division, and present common manifestations like inflammatory events, squamous lesions, skin discomfort, and pronounced damage at sun exposure, impacting the psycho-social life quality of the individuals (Richard *et al.*, 2022; Dreno *et al.*, 2021).

Salicylic acid (SA), a classic β -hydroxy acid with evidenced therapeutic applications, contributes to the healing of mild cutaneous lesions as a function of concentration, being a constituent of a broad range of dermatocosmetic products due to anti-inflammatory, antimicrobial, exfoliating, and anti-seborrheic properties. Additional benefits of using SA are UV protection and reduction of erythematous reaction through protein transcription inhibition (Kornhauser *et al.*, 2010). Recent evidence conceived in the demonstration of melanogenesis inhibition of SA from ginseng root, and anticancer activity in skin melanoma (Liu *et al.*, 2021; Ausina *et al.*, 2020). Several attempts were conducted to study SA solubilization, as

key compound in the formulation of nano-sized medication for treating acne, psoriasis, warts or combined with a second drug to improve anti-inflammatory, keratolytic, or antibacterial activity (Anicescu *et al.*, 2022, Seviñç Özakar *et al.*, 2022).

There is a high interest in studying microemulsions (MES) for topical application of dermatologic drugs. Known as thermodynamically stable and isotropic nanodispersions, oil in water (O/W) MES possess an enhanced capacity of solubilizing and entrapping lipophilic drugs into an oil core stabilized in an aqueous media with the aid of a surfactant and a cosurfactant (Talianu *et al.*, 2019).

The objective of this study followed the development and characterization of topical microemulsions with SA solubilized into an oil phase, intended to be applied in the treatment of dermatologic conditions known to create imbalances in normal cellular metabolism.

MATERIALS AND METHODS

Materials

Salicylic acid was acquired from Chemical Company, oleic acid vegetable from Merck, Tween 80 from Carl Roth, propylene glycol (PG) from Sigma Aldrich, Ultrapure Milli-Q water was generated from a Milly-Q® Direct 8 Water Purification System (Merck Millipore), being the aqueous phase.

Methods

Design of the Pseudoternary Phase Diagrams

To prepare stable O/W microemulsions entrapping salicylic acid it was mandatory to study the stability areas of the O/W and W/O microemulsions, of some lamellar phases and unstable regions. For a chosen ratio of Tween 80/PG of 2:1, nine different oil/stabilizer mixture dilution lines of 1:9, 2:8, 3:7, 4:6, 5:5, 6:4, 7:3, 8:2, and 9:1 were considered to explore the formation of microemulsions using water titration method. The diagram was plotted using Triplot 4.1.2. (Todd Thompson Software, LA, USA). All dispersions were inspected and six stable points of microemulsions were chosen as it shows in Figure 1.

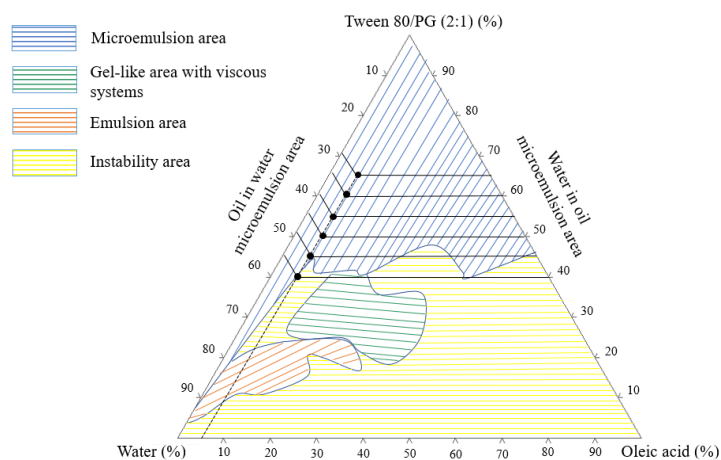


Figure 1. Pseudoternary phase diagram built to explore the formation of MEs

Preparation of the O/W Microemulsions

Following the data presented in Table 1, the calculated quantity of salicylic acid was accurately weighed at a Sartorius MC1 Laboratory LC 620 P analytical balance (Sartorius, Gottingen, Germany), and solubilized in oleic acid under magnetic stirring using DLAB MS-H380Pro thermostated stirrer (DLAB Scientific, Beijing, China). Afterward, the mixture of Tween 80 and PG (in a ratio of 2:1) was slowly added to the oily dispersion. The homogenization was continued, and the preparation process was succeeded by adding distilled water through meticulous titration until 20 g of microemulsion was obtained. The resulting dispersions were left to equilibrate for 24 hours and further characterized.

Table 1. Composition of the O/W microemulsions

Ingredients (w/w, %)	MES 1	MES 2	MES 3	MES 4	MES 5	MES 6
Oleic acid	5	5	5	5	5	5
Tween 80/PG (2:1)	40	45	50	55	60	65
Salicylic acid	1	1	1	1	1	1
Distilled water	54	49	44	39	34	29

pH Determination

The pH of the microemulsions was evaluated using a Mettler Toledo pH meter (Mettler-Toledo GmbH, Greifensee, Switzerland).

Conductivity Determination

The conductivity of the microemulsions was assessed to confirm their phase behavior. Corning 441 conductivity meter (Cole Parmer, Vernon Hills, USA) was used, and the measurements were recorded in triplicate, at 24 ± 0.5 °C.

Refractive Index Determination

The refractive index of the microemulsions was obtained using a Krüss DR 201-95 digital refractometer (Krüss Optronic, Hamburg, Germany). Distilled water with a refractive index of 1.3330 was used to calibrate the apparatus. The measurements were recorded in triplicate at 24 ± 0.5 °C.

Dynamic Light Scattering Determination (DLS)

The mean droplet size and the polydispersity index (PDI) were assessed using DLS technique on diluted samples (Talianu *et al.*, 2024). VascoKin particle analyzer (Cordouan Technologies, Pessac, France), equipped with a 638-nanometer laser functioning in a backscattering mode was used over the analysis process to explain droplet behavior using the Cumulant and Sparse Bayesian Learning (SBL) algorithm.

Rheological Evaluation

The flow behavior of the microemulsions was studied using a rotational viscometer, Multi-Visc Rheometer (Fungilab, Barcelona, Spain) (Dănilă *et al.*, 2024), equipped with an LCP standard spindle at 24 ± 0.5 °C. The operational conditions were previously reported (Anicescu *et al.*, 2022).

Superficial Analysis

The surface tension of the microemulsions was tested with a Sigma 700 force tensiometer in quinduplicate mode (Biolin Scientific, Finland) (Hamed *et al.*, 2022). Under the guidance of Du Noüy ring method, the platinum ring interacted with the microemulsion sample measuring the maximum force of detachment at the liquid surface.

RESULTS AND DISCUSSION

The organoleptic characteristics of the microemulsions translated as aspect, color and odor were associated with the composition. From Figure 2 it can be seen that the microemulsions presented different aspects from opalescent to transparent appearance, being observed how the stabilizer mixture affects their internal structure.



Figure 2. Microemulsions observed at 24 h after preparation

The pH values varied in the range 2.90 ± 0.01 - 3.51 ± 0.01 , being strongly influenced by the presence of acidic species of salicylic acid and oleic acid, and gradually increased to the maximum value with the increase in the stabilizer content.

Conductivity evaluation confirmed the O/W type of the microemulsions. The experimental values ($\mu\text{S}/\text{cm}$) varied between 48.30 ± 0.10 - $104.27 \pm 0.15 \mu\text{S}/\text{cm}$ as a function of the aqueous phase content. Similarly, the refractive index increased with the S/CoS concentration from 1.3750 ± 0.0001 to 1.4175 ± 0.0001 , giving information about the isotropic character. Preliminary analysis results performed in triplicate can be followed herein in Table 2.

Table 2. Experimental data of pH, conductivity and refractive index obtained in the preliminary analysis of microemulsions

Code	pH	Conductivity	Refractive index
MES 1	2.90 ± 0.01	104.27 ± 0.15	1.3750 ± 0.0001
MES 2	3.02 ± 0.01	102.53 ± 0.12	1.3848 ± 0.0001
MES 3	3.04 ± 0.00	99.17 ± 0.51	1.3856 ± 0.0000
MES 4	3.26 ± 0.01	83.90 ± 0.56	1.4050 ± 0.0001
MES 5	3.35 ± 0.00	66.17 ± 0.31	1.4096 ± 0.0001
MES 6	3.51 ± 0.00	48.30 ± 0.10	1.4175 ± 0.0001

During dynamic light scattering analysis, the mean droplet size and droplet size distribution were assessed following two methods as presented in Table 3. According to the Rayleigh theory of light scattering, the logarithmic autocorrelation function of intensity in time (μs) was obtained to calculate the diffusion coefficient and the mean droplet size by applying the Stokes-Einstein equation.

Table 3. Cumulative results obtained over the DLS analysis, presenting the mean droplet size values processed by the Cumulant and the SBL models

Code	Z_{average} (nm)	PDI	Cumulant Model			Sparse Bayesian Learning model		
			D _{10%} (nm)	D _{50%} (nm)	D _{90%} (nm)	D _{10%} (nm)	D _{50%} (nm)	D _{90%} (nm)
MES 1	272.73	0.390	215.44	451.46	946.03	102.81	472.82	716.84
MES 2	218.82	0.322	170.97	326.63	653.52	107.68	297.78	623.99
MES 3	208.59	0.325	163.25	311.87	623.99	889.50	297.78	750.60
MES 4	160.71	0.295	135.68	259.21	495.20	74.39	179.07	716.84
MES 5	130.85	0.272	98.17	187.57	358.28	64.75	163.25	375.23
MES 6	117.50	0.290	98.17	187.54	358.28	53.82	163.25	225.64

With the aid of the Cumulant model, Z_{average} values of the mean droplet size were obtained together with the PDI. As it was valued in Figure 3 presenting the dynamics of droplet size distribution - case (a), the droplet diameter was influenced by composition. The increase in S/CoS (%) determined a decrease in droplet size from 272.73 nm to 117.5 nm. Moreover, the size distribution was well represented by D10%-D90% domains as presented in Table 3, where the best results were attributed to the MES 5 and MES 6 systems. At concentrations of 60-65% Tween 80/PG (%), the corresponding peaks were shifted towards 100 nm.

Because it is hard to find samples with a single monodispersed domain of droplets, a variation in droplet size distribution can be emphasized using a continuous multimodal analysis algorithm. Considering the variation of PDI between 0.272 and 0.390, it was worthwhile to make a SBL analysis. Thus, the droplet size distribution was quantified as well through D10%-D90% domains and graphically represented in Figure 3 - case (b).

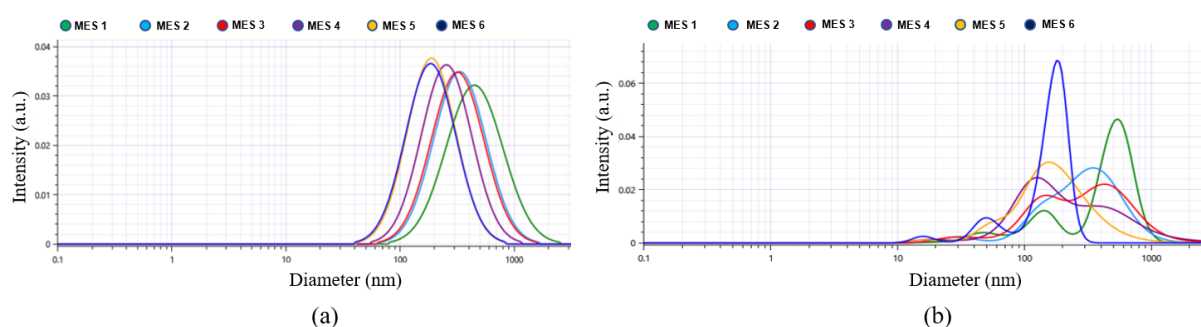


Figure 3. Cumulative profiles of intensity (a.u.) as a function of diameter (nm) analyzed based on Cumulant model - case (a), and profiles of intensity (a.u.) as a function of diameter (nm) analyzed based on SBL model – case (b).

It can be noticed a good result for MES 6, where the high-intensity peak was placed between 100-200 nm, followed by low-intensity peaks under 100 nm, reflecting the existence of small droplets with trimodal distribution. The droplet size diameter represents in this way an important parameter to predict the behavior of the microemulsions in topical application and consequently, the drug passage through skin pathways.

Recent studies centered on cosmetic emulsions development found that the rheological profile is influenced by the stabilizer activity. It was stated that the stabilizer (S/CoS) is a determinant component for stability and spreadability, and together with the bioactive ingredients, contributes to an adequate application at the skin level (Dănilă *et al.*, 2019).

Over the rheological evaluation, non-Newtonian and Newtonian flows were assessed, being strongly connected with the variation in droplet size distribution. Rheological profiles of the shear stress (Pa) as a function of shear rate (s^{-1}) were presented in Figure 4, while the rheological descriptors can be seen in Table 4. MES 1 - MES 3 followed a pseudoplastic flow, described by the Ostwald-de Waele model for MES 1 with consistency index (K) values of $0.937 Pa \cdot s^n$, while in the case of MES 2 and MES 3, the Herschel-Bulkley model was quantified by elevated K values with τ_0 of 1.343 Pa and 2.782 Pa (Figure 4 - case (a)).

Corroborating the viscosity with the droplet size variation, the three nanodispersions behaved as fluid emulsion-like systems with larger droplets over 500 nm and pseudoplastic behavior.

At a constant concentration of the oil phase, the increase in stabilizers S/CoS (Tween 80/PG) determined a reduction in droplet size, and a different rheological behavior resulting in clear microemulsions with a laminar flow.

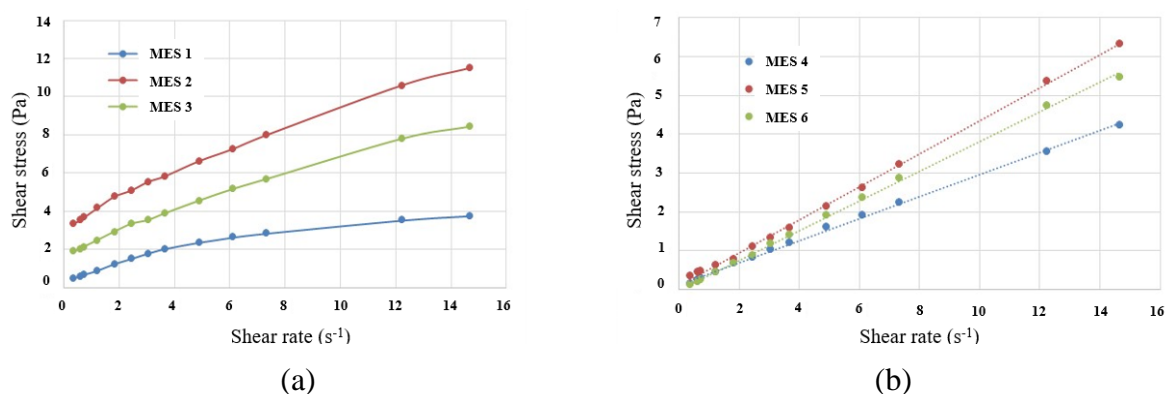


Figure 4. Rheological profiles of shear stress (Pa) as a function of shear rate (s^{-1}) for the tested MES 1 – MES 6 at $24 \pm 0.5^\circ C$ representing the non-Newtonian flow (a) and Newtonian flow behavior (b)

Consequently, the Newtonian profiles of the MES 4 - MES 6 nanodispersions presented in Figure 4 – case (b) were described by viscosity values between 0.283 and 0.424 Pa·s, unaffected by the variation of shear stress and shear rate. The model was well fitted by regression coefficients placed between 0.9991 and 0.9995, as mentioned in Table 4. The values obtained in this case are closely related to the results reported in the literature, as recently emphasized for an optimized methotrexate topical microemulsion with a viscosity of 0.103 Pa·s and Newtonian flow (Mishra *et al.*, 2024).

The most elevated viscosity values were recorded for MES 2 and MES 3 and can be justified by the flow behavior transitions observed on the phase diagram.

Table 4. Rheological descriptors for the non-Newtonian and Newtonian flow behavior of the tested microemulsions

Code	Model	R	τ_0 (Pa)	K, ($Pa \cdot s^n$)/ viscosity (Pa·s)	n
MES 1	Ostwald-de Waele	0.9929	0	0.937	0.534
MES 2	Herschel-Bulkley	0.9995	2.782	1.178	0.747
MES 3	Herschel-Bulkley	0.9994	1.343	0.993	0.738
MES 4	Newton	0.9991	0	0.2836	1
MES 5	Newton	0.9993	0	0.4241	1
MES 6	Newton	0.9995	0	0.3815	1

The surface tension of the microemulsions placed around 30.825 ± 0.008 mN/m and 34.710 ± 0.503 mN/m indicated the formation of stable systems, with minimal values obtained for MES 4 – MES 6 prepared with the highest S/CoS amount. The results are graphically presented in Figure 5. The reduction in surface tension promoted by the S/CoS mixture allows appropriate spreading onto a surface, facilitating the microemulsion application on the skin area and the enhanced formulation activity at the cellular level.

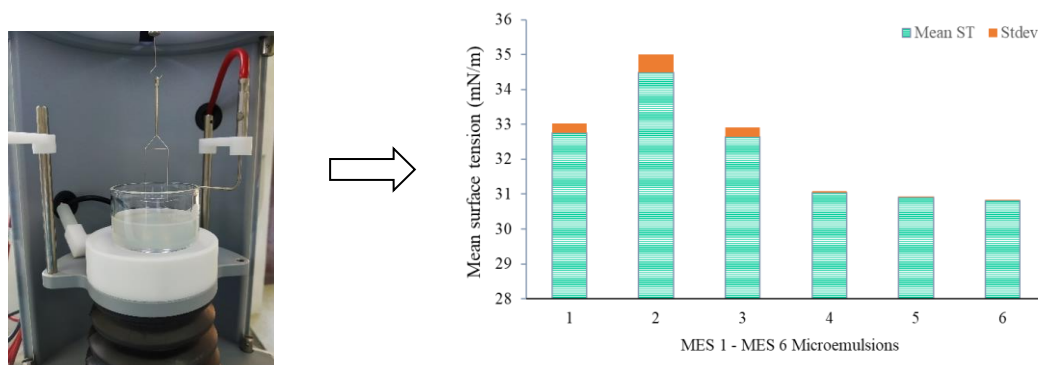


Figure 5. Variation of surface tension for the tested MES 1 - MES 6 at $24 \pm 0.5^\circ\text{C}$, analyzed with Du Noüy ring method

It can be appreciated that the obtained data offer important information concerning the stability of the interfacial film at the oil/water interface, as previously explained in the case of surfactant migration phenomena from the interface (Koli *et al.*, 2021), on the rule the smaller the surface tension variation, the higher the stability will be.

CONCLUSIONS

The obtained microemulsions were stable and the composition appropriately influenced their physicochemical parameters. The designed systems can be used as solubilizing vehicles for salicylic acid by selecting suitable oil phases and stabilizers in calculated amounts, using pseudoternary phase diagram plotting. The physical parameters analyzed over the experimental process, namely conductivity, refractive index, droplet size, rheological behavior, and surface tension lead to the depiction of two model microemulsions. Thus, the MES 5 and MES 6 had reduced droplet sizes of 130.85 nm and 117.50 nm, respectively, according to the Cumulant model, with the lowest PDI values. The SBL algorithm contributed to the droplet dynamics understanding and identification of different droplet populations leveraging the system stability. As fluid systems, described by Newtonian flow and low surface tension, a targeted effect and adequate skin contact allow the drug passage. To conclude, the designed microemulsions could be emphasized as potential systems of interest in the current management of dermatologic conditions.

Acknowledgements

This paper was financially supported by the Carol Davila University of Medicine and Pharmacy Bucharest, Romania, through Contract No. CNFIS-FDI-2024-F-0570.

REFERENCES

- Anicescu, M.-C., Dinu-Pîrvu, C.-E., Talianu, M.-T., Ghica, M.V., Anuța, V., Prisada, R.M., Nicoară, A.C. & Popa, L. (2022). Insights from a Box-Behnken Optimization Study of Microemulsions with Salicylic Acid for Acne Therapy. *Pharmaceutics*, 14(1), 174. <https://doi.org/10.3390/pharmaceutics14010174>
- Dănilă, E., Kaya, D.A., Anuța, V., Popa, L., Coman, A.E., Chelaru, C., Constantinescu, R.R. Dinu-Pîrvu, C.-E., Albu Kaya, M.G. & Ghica, M.V. (2024). Formulation and Characterization of Niacinamide and Collagen Emulsion and Its Investigation as a Potential Cosmeceutical Product. *Cosmetics*, 11(2), 40, <https://doi.org/10.3390/cosmetics11020040>, ISSN 2079-9284
- Dănilă, E., Moldovan, Z., Albu Kaya, M.G. & Ghica, M.V. (2019). Formulation and Characterization of Some Oil in Water Cosmetic Emulsions Based on Collagen Hydrolysate and Vegetable Oils Mixtures. *Pure and Applied Chemistry*, 91(9), 1493-1507. <https://doi.org/10.1515/pac-2018-0911>, ISSN 0033-4545
- Dreno, B., Amici, J.M., Demessant-Flavigny, A.L., Wright, C., Taieb, C., Desai, S.R. & Alexis, A. (2021). The Impact of Acne, Atopic Dermatitis, Skin Toxicities and Scars on Quality of Life and the Importance of a Holistic Treatment Approach. *Clinical, Cosmetic and Investigational Dermatology*, 14, 623–632. <https://doi.org/10.2147/CCID.S315846>
- Hamed, R., Abu Kwiak, A.D., Al-Adhami, Y., Hammad, A.M., Obaidat, R., Abusara, O.H. & Huwajj, R.A. (2022). Microemulsions as Lipid Nanosystems Loaded into Thermoresponsive *in situ* Microgels for Local Ocular Delivery of Prednisolone. *Pharmaceutics*, 14(9), 1975. <https://doi.org/10.3390/pharmaceutics14091975>
- Koli, A.R., Ranch, K.M., Patel, H.M., Parikh, R.K., Shah, D.O. & Maulvi, F.A. (2021). Oral Bioavailability Improvement of Felodipine Using Tailored Microemulsion: Surface Science, *ex vivo* and *in vivo* Studies. *International Journal of Pharmaceutics*, 596, 120202. <https://doi.org/10.1016/j.ijpharm.2021.120202>
- Kornhauser, A., Coelho, S.G. & Hearing, V.J. (2010). Applications of Hydroxy Acids: Classification, Mechanisms, and Photoactivity. *Clinical, Cosmetic and Investigational Dermatology*, 3, 135–142. <https://doi.org/10.2147/CCID.S9042>
- Liu, J., Jiang, R., Zhou, J., Xu, X., Sun, Z., Li, J., Chen, X., Li, Z., Yan, X., Zhao, D., Zheng, Z. & Sun, L. (2021). Salicylic Acid in Ginseng Root Alleviates Skin Hyperpigmentation Disorders by Inhibiting Melanogenesis and Melanosome Transport. *European Journal of Pharmacology*, 910, 174458, <https://doi.org/10.1016/j.ejphar.2021.174458>
- Mishra, M., Barkat, M.A., Misra, C., Alanezi, A.A., Ali, A., Chaurawal, N., Ali, A., Preet, S., Barkat, H. & Raza, K. (2024). Lipid-based Microemulsion Gel for the Topical Delivery of Methotrexate: An Optimized, Rheologically Acceptable Formulation with Conducive Dermatokinetics. *Archives of Dermatological Research*, 316(6), 316, 1–17, <https://doi.org/10.1007/s00403-024-03140-8>
- Richard, M.A., Paul, C., Nijsten, T., Gisondi, P., Salavastru, C., Taieb, C., Trakatelli, M., Puig, L., Stratigos, A. & EADV Burden of Skin Diseases Project Team (2022). Prevalence of Most Common Skin Diseases in Europe: A Population-Based Study. *Journal of the European Academy of Dermatology and Venereology*, 36(7), 1088–1096. <https://doi.org/10.1111/jdv.18050>
- Seviñç Özakar, R., Asan, Ş., Özkan, A.E. & Özakar, E. (2022). Preparation and Characterization of Combined Salicylic Acid and Povidone-Iodine Containing Nanoemulgels: A Preliminary Study. *Journal of Faculty of Pharmacy of Ankara University*, 46(3), 764-780. <https://doi.org/10.33483/jfpau.1137486>
- Talianu, M.-T., Dinu-Pîrvu, C.-E., Ghica, M.V., Anuța, V., Jinga, V. & Popa, L. (2019). Foray into Concepts of Design and Evaluation of Microemulsions as a Modern Approach for Topical Applications in Acne Pathology. *Nanomaterials*, 10(11), 1-43. <https://doi.org/10.3390/nano10112292>
- Talianu, M.-T., Dinu-Pîrvu, C.-E., Ghica, M.V., Anuța, V., Prisada, R.M. & Popa, L. (2024). Development and Characterization of New Miconazole-Based Microemulsions for Buccal Delivery by Implementing a Full Factorial Design Modeling. *Pharmaceutics*, 16(2), 271. <https://doi.org/10.3390/pharmaceutics16020271>
- Zhang, J., Zhong, F., He, K., Ji, M., Li, S. & Li, C. (2023). Recent Advancements and Perspectives in the Diagnosis of Skin Diseases Using Machine Learning and Deep Learning: A Review. *Diagnostics (Basel, Switzerland)*, 13(23), 3506. <https://doi.org/10.3390/diagnostics13233506>